# Progress in Development of Reconfigurable Intelligent Surfaces with Liquid-Crystal and Glass Substrates for RF Applications

*Changhyeong Lee*, Hyengcheul Choi, Jaewon Huh, Boyoung Kang, and Byounggwan Kang*
***Corning Technology Center Korea (CTCK), Asan-si, Chungcheongnam-do, Republic of Korea**

## Abstract
*Reconfigurable intelligent surfaces (RIS) is an alternative solution to overcome the drawbacks of mmWave and upper-mid carrier frequencies for 5G/6G wireless communications. RIS has become the talk of the town. Its main purpose is to maintain a line-of-sight status through new propagation paths. To realize this function in real time, a tunable element is required. By utilizing the change in characteristics of dielectrics according to voltage variation, liquid crystal (LC) materials can be used as the tunable element in the electromagnetic domain. The LC materials are used to push the envelope by reducing complexity, manufacturing costs, and path loss from incumbent semiconductor-based active devices. This paper addresses our step-by-step approach to developing advanced active RIS, which are thinner and larger. Our first proof-of-concept sample started with a 200 μm-thick cell gap at a size of 80×80 mm², and now we have a 20 μm-thick cell gap at the size of Gen2 glass. From the first to the present samples, we have dramatically reduced response time and driving voltage levels (from tens of seconds to several milliseconds and from double-digit voltages to single-digit voltages) with innovative design changes and optimizations, as the cell gap has been reduced from 200 to 20 μm.*

## Author Keywords
Liquid crystal; reconfigurable intelligent surfaces; beam steering; reflector; 5G; mmWave; Ka-band; glass-embedded; driving voltage; Radio frequency;

## 1. Introduction

Millimeter-wave (mmWave) and upper-mid bands utilized for 5G/6G wireless communications suffer from higher path loss and smaller coverage due to their characteristics of short wavelength and straight-line propagation [1, 2]. To mitigate these drawbacks, high-gain phased array antennas have been proposed. However, the gain of phased array antennas is limited by the aperture efficiency and the feeding network within the constrained space of transceivers [3]. Additionally, even with these solutions, obstacles between a base station and mobile terminals remain unavoidable. To address this issue, numerous studies have been published on securing line-of-sight (LoS) for high-quality signals using reconfigurable intelligent surfaces (RIS). RIS can create new communication links between base stations and users [4]. Figure 1 illustrates the basic concept of RIS for next-generation wireless communications. With real-time beam steering, RIS can provide a seamless network solution, even when the location of users and the communication environment change instantaneously. Extensive research is being conducted in this field [5-9]. To achieve the tunability of RIS, PIN diode-driven RIS has been proposed. However, a unit cell with a PIN diode requires multiple diodes to achieve multi-bit (> 2-bits) beam-steering functions. Multiple DC lines and vias increase the design complexity of this structure.

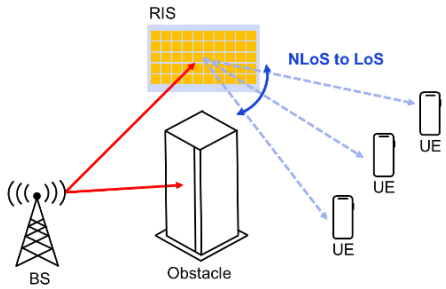


**Figure 1**. Example of creating new propagation pathways using active RIS

To alleviate the shortcomings of conventional RIS with semiconductor-based devices, researchers [6-9] have proposed reconfigurable mmWave devices based on liquid crystals (LC). These studies investigate the manipulation of the reflection angle by modulating the phase of reflection in the unit cells. They achieve this by changing the dielectric constant according to the driving voltage, which enables continuous phase shifting. By leveraging this characteristic of LC, RIS can achieve real-time beam steering in the microwave region. In addition to these RF characteristics of LC, utilizing LC allows for reduced manufacturing costs by using existing LCD mass production (MP) lines. LC also offers scalability with larger glass substrates compared to PCBs. Despite these advantages, ongoing research is needed on thin cell gaps and large footprints to achieve fast response speeds, low operating voltages, low spillover losses, and reduced LC material costs.
In this paper, we explain and summarize our step-by-step approach to developing advanced active RIS using LC material, focusing on creating thinner and larger RIS. From the first proof-of-concept sample to the current advanced sample, we have achieved several benefits with larger sized glass (370×470 mm²) and thinner cell gaps (20 μm). These advantages include wide and precise beam steering angles, minimal spillover losses, high directivity, faster response times (<1 second), and lower driving voltage levels (single-digit). As a result of these pragmatic approaches, we anticipate that LC-based active RIS will become a strong candidate for addressing the challenges posed by high-frequency bands in next-generation communications.

## 2. Evolutionary LC RIS design

A. Continuous controlled RIS Concept with thick LC medium

The proposed LC RIS structure is illustrated in Figure 1(a). The RIS consists of 12×12 identical unit cells, each containing a circular patch with a radius of 1.45 mm, designed to resonate at the Ka-band. The total area of the RIS is 80×80 mm². Each unit cell has an area of 5×5 mm², with a minimum distance of 2.1 mm between adjacent circular patches. The structure comprises two Corning glass sheets (500 μm thick), a liquid crystal (LC) layer (Merck GT7-29001, 100 μm thick), and two metal layers (copper,


ISSN 0097-996X/25/5602-1294-$1.00 © 2025

600 nm thick). The effective dielectric constant and loss tangent of the LC at 19 GHz vary from 2.46 to 3.53 and from 0.0064 to 0.0116, respectively. These results depend on the strength of the perpendicular electric field within the LC cell, which is proportional to the amplitude of the bias voltage. Figure 1(b) shows the reflection phases of the proposed unit cell as the dielectric constant of the encapsulated LC layer varies. Full-wave simulations indicate that the achievable reflection phase range is 252°, with an operating bandwidth exceeding 800 MHz.

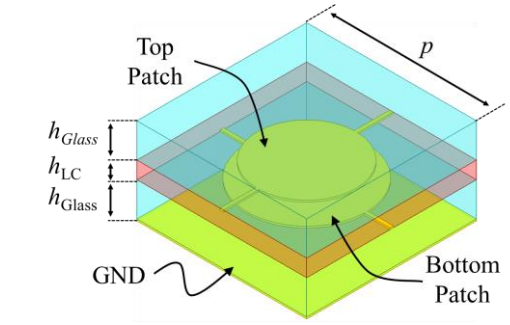


(a)

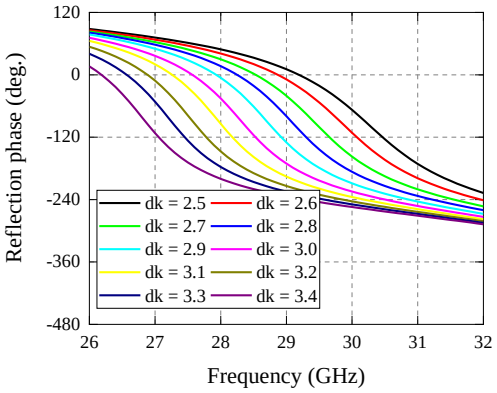


(b)

**Figure 2**. Proposed unit-cell structure of LC RIS with 100 μm cell gap (a) physical dimension (b) simulated phases of $S_{11}$ in degree according to the variation of the dielectric constant

B. 1-bit quantization-controlled LC RIS concept with a thin 20 um active medium

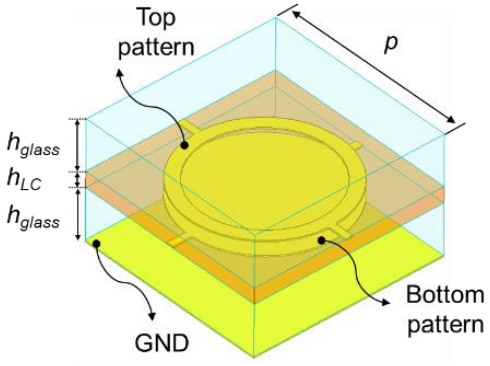


(a)

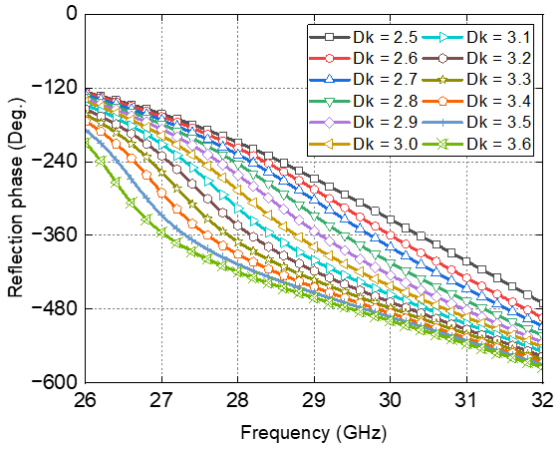


(b)

**Figure 3**. Proposed unit-cell structure of LC RIS with a 20 μm cell gap (a) physical dimension (b) simulated phases of $S_{11}$ in degree according to the variation of the dielectric constant

Figure 3(a) depicts the unit-cell structure of the proposed LC RIS with a 20 μm cell gap. The proposed unit-cell for the RIS has an area of 2.7×2.7 mm² (the period of the proposed unit-cell is 2.7 mm, approximately λ/4), forming a ring with a diameter of 2.1 mm to resonate at the Ka-band. The overall structure is the same as the previous design, with the only changes being the thicknesses of the glass and the LC (the glass is 700 μm thick and the LC cell gap is 20 μm thick). Based on the unit-cell design, the proposed RIS was fabricated with a periodic 48×48 array of unit-cells, covering a total area of 150×150 mm². To drive the LC between the two glass sheets, the driving voltage lines are designed on the top and bottom glass layers. Figure 3(b) shows the reflection phases of the proposed unit-cell design as the dielectric constant of the encapsulated LC varies. As the dielectric constant increased from 2.5 to 3.6, a change in the reflection phase of more than 180° was confirmed over a 1.5 GHz bandwidth centered at 28 GHz. The designed unit-cell was simulated using a commercial full-wave simulation tool. The frequency responses of the unit-cell were obtained through a periodic boundary condition analysis with a variation of the dielectric constant (from 2.5 to 3.5) using nematic LC. For 1-bit quantization beam steering, the designed unit-cell has a phase shift range of the reflection coefficient exceeding 180°. Additionally, the unit-cells were optimized for the lowest reflection loss at each dielectric constant, achieving a 180° phase difference and minimizing the difference in reflection loss between the two states.

**Table 1.** Comparison between 100 μm and 20 μm cell gap

| Item | #1 | #2 |
|---|---|---|
| Glass thickness | 500 μm (pair) | 700 μm (pair) |
| LC thickness | 100 μm | 20 μm |
| Unit-cell | Circles | Ring & circle |
| Phase variation | > 300° | > 200° (1-bit) |
| Response time | 18 sec (turn-off) | 130 ms (turn-off) |
| Driving voltage level | 0-5V | 0-20V |

## 3. Fabrication and Experiments

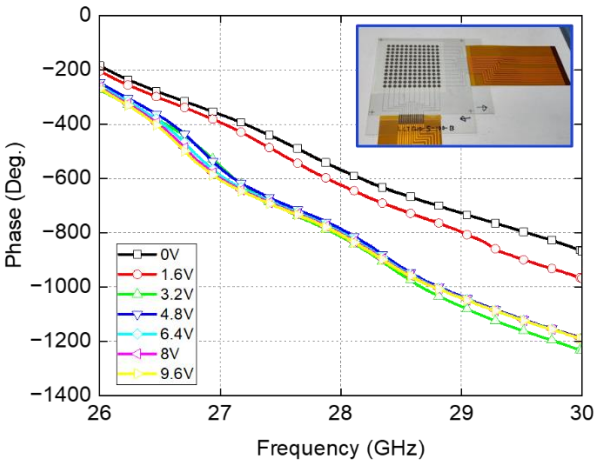


(a)

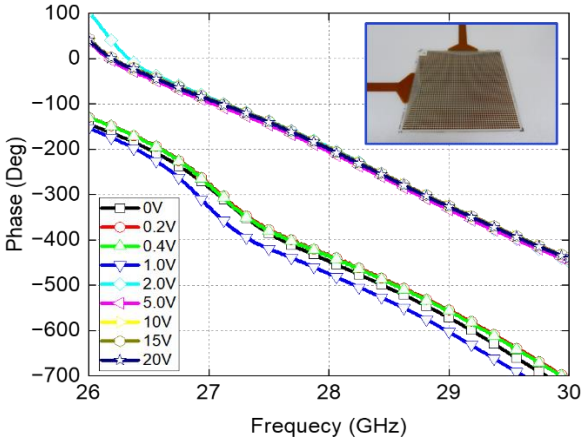


(b)

**Figure 4**. Measured dynamic range of phase variation according to driving voltage levels and a photograph of the fabricated RIS with (a) 100 μm cell gap (b) 20 μm cell gap

Figures 4(a) and 4(b) show photographs of the fabricated LC RIS samples with 100 μm and 20 μm cell gaps, respectively. FPCBs are used to input the driving voltage on the right and bottom edges of the LC RIS samples. The physical dimensions of the fabricated samples are in good agreement with the designed specifications. The RF performance of the fabricated LC RIS at the target frequency band is also satisfactory, as shown in Figures 4(a) and 4(b). The magnitude and phase of the RIS reflection coefficient were measured using a PNA network analyzer (Keysight, N5224B). Unlike the simulations, real-life measurements of the RF performance for the unit cell were conducted with a horn antenna operating in the mmWave band, which was placed on the top surface of the RIS. To examine the maximum tunability, the bias voltage was increased up to 25V across all the copper patterns on the top glass, while all the copper patterns on the bottom glass were connected to ground. The measured tunability range is 14.1% (28.9-33.3 GHz), which is similar to the simulation results for the 100 μm-thick cell gap design. For the 100 μm-thick cell gap, the measured dynamic range of phase appears to be larger than 250° at 27-30 GHz, which can achieve 1-bit quantization for beam steering as an active RIS. The prototype's threshold voltage is around 3V to change the phase of reflection in the target frequency band. The frequency response to the amplitude of the bias voltage is almost saturated around 10V in both cases.

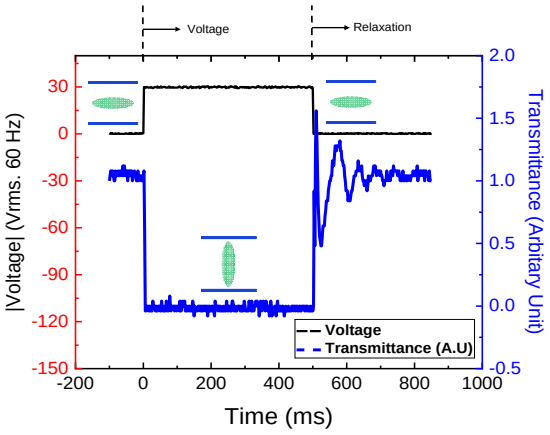


**Figure 5**. Response time of the proposed active LC RIS device

Figure 5 presents an electro-optical analysis of our proposed LC RIS device under crossed polarizers, specifically for measuring the turn-on and turn-off response times. The conventional 100 μm thick LC RIS device exhibits a prolonged total response time of 20 seconds, primarily relying on slow relaxation mechanisms during turn-off. In contrast, our innovative design, featuring a cell-gap reduced to one-fifth of the conventional thickness (only about 20 μm), achieves an exceptional total response time of only 130 ms.

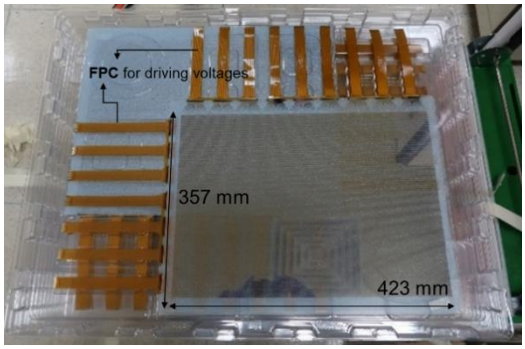


**Figure 6**. Fabricated Gen2 size active LC RIS

To achieve low spillover loss and high directivity (suppressing sidelobes), we have developed a Gen2 size active RIS, surpassing the performance of smaller active RIS. Figure 6 shows the fabricated Gen2 size active LC RIS sample. The overall size of the RIS is 370×470 mm² (Gen2 size glass) and it consists of a 112×144 array of unit cells. Each unit cell is grouped into 16 units and arranged in a 7×9 grid to control the RIS using driving voltages with FPCB.

**Table 2.** Comparison of our evolutionary active LC RIS

| | Size | # of unit-cell | RCS gain [dB] |
|---|---|---|---|
| #1 | 80×80 mm$^2$ | 12×12 | 52 dB |
| #2 | 150×150 mm$^2$ | 48×48 | 65 dB |
| #3 | 370×470 mm$^2$ | 112×144 | 84 dB |

Table 2 provides a comparison of our developed active LC RIS. As shown in the table, our active LC RIS has undergone step-by-step changes and evolution. Finally, based on our prior experiences, we have designed and fabricated the world's first Gen2 size active LC RIS. As a result, the proposed Gen2 size RIS has a larger radar cross section (RCS) gain, which represents the strength of the reflected signal (in dB) from the target/object in the radar receiver direction when compared to a standard reflector, such as smooth spheres or rectangular objects. Additionally, it exhibits a faster response time compared to previous works.

## 4. Conclusion

In this paper, we have described our evolutionary progress in the development of an active LC RIS for RF applications. To achieve fast response times, low spillover-loss, and low driving voltage levels, we are developing advanced active RIS with thinner and larger dimensions. As the first step, we began with a cell gap of 200 μm at a size of 80×80 mm². In the second stage, we developed a cell gap of 100 μm while maintaining the same size of 80×80 mm². In the third phase, we created an RIS with a 20 μm-thick cell gap at an increased size of 150×150 mm². Finally, we fabricated the world's first Gen2 RIS with dimensions of 370×470 mm². Throughout these stages, we have significantly reduced the response time and driving voltage level—from tens of seconds to several milliseconds and from double-digit to single-digit voltages. These improvements were achieved through innovative design changes and optimizations as the cell gap decreased from 200 to 20 μm. With these advancements, we believe our RIS technology can be a viable solution for ensuring seamless wireless communication in complex indoor and outdoor environments, particularly in the mmWave bands. The reduction in response time and driving voltage makes our RIS a promising candidate for both overcoming obstacles and enhancing connectivity.

## 5. References

[1] Theodore S. Rappaport et al., "Millimeter Wave Mobile Communications for 5G Cellular: It Will Work!,"IEEE Access, vol. 1, pp. 335-349, 2013.

[2] 5G Evolution and 6G, NTT DoCoMo, Tokyo, Japan, 2020.

[3] Oh J, Thiel M, and Sarabandi K, "Wave-propagation management in indoor environments using micro-radio-repeater systems, " IEEE Antennas and Propagation Magazine, vol. 52, no. 2, pp. 76-88, 2014.

[4] 6G the Next Hyper-Connected Experience for All, Samsung Res., Samsung Electron., Suwon-si, South Korea, 2021.

[5] J. Jeong, J. H. Oh, S. Y. Lee, Y. Park and S. -H. Wi, "An Improved Path-Loss Model for Reconfigurable-Intelligent-Surface-Aided Wireless Communications and Experimental Validation," IEEE Access, vol. 10, pp. 98065-98078, 2022.

[6] Hogyeom Kim et al, "Independently Polarization Manipulable Liquid Crystal-Based Reflective Metasurface for 5G Reflectarray and Reconfigurable Intelligent Surface," IEEE Transactions on Antennas and Propagation, vol. 71 no. 8, 2023.

[7] Zhang, Weiquan, Yue Li, and Zhijun Zhang. "A Reconfigurable Reflectarray Antenna with an 8-μm-thick Layer of Liquid Crystal," IEEE Transactions on Antennas and Propagation, 2021.

[8] Byounggwan Kang et al., "Tunability of Reconfigurable Intelligent Surface (RIS) using Liquid Crystal (LC) according to Various Voltage Levels," SID Symposium Digest of Technical Papers, vol. 54, no. 1, pp. 993–996, 2023.

[9] Youngno Youn, Donggeun An, Daehyeon Kim, Myeonggin Hwang, Hyengcheul Choi, Byounggwan Kang, and Wonbin Hong, "Liquid Crystal-driven Reconfigurable Intelligent Surface with Cognitive Sensors for Self-Sustainable Operation," IEEE Transactions on Antennas and Propagation, 2023.

[10] Changhyeong Lee et al., "A Novel Design for RIS with Thin LC Layer for Wireless Communications," SID Symposium Digest of Technical Papers, 55(1), 208–211, (2024).

[11] Boyoung Kang et al., "Active Reconfigurable Intelligent Surface Utilizing Liquid Crystal for 5G Communication," The 23rd International Meeting on Information Display, C35-1, (2023).

[12] Jaewon Huh et al., "Development of An Active Reconfiguration Intelligent Surfaces Based on Thin Liquid Crystal Medium," The 24th International Meeting on Information Display, F54-5, (2024).